



1 *Keywords:* cosmogenic nuclides; weathering; soil production; saprolite; rock strength

2

### 3 **1. Introduction**

4           Analyses of in-situ-produced cosmogenic nuclides, especially  $^{10}\text{Be}$  ( $T_{1/2} =$   
5  $1.36 \times 10^6$  yr) and  $^{26}\text{Al}$  ( $T_{1/2} = 7.05 \times 10^5$  yr) produced in quartz, have revolutionized our  
6 approach to the dating of landforms and determining the rates of earth surface processes  
7 (Gosse and Phillips, 2001). The application of the cosmogenic nuclide methods in  
8 geomorphology has altered our understanding of the ages of landforms and the  
9 timescales of landscape change (Bierman et al., 2002; Bierman and Nichols, 2004;  
10 Cockburn and Summerfield, 2004; Von Blanckenburg, 2006). Such nuclides can be used  
11 as a chronometer that provides the exposure age of an ‘event surface’, where both of  
12 pre-exposure nuclide accumulation under the depths of shielding and post-exposure  
13 erosion is negligible. The nuclide concentration at an actively eroding surface or in  
14 sediment eroded from its source area acts as an indicator of denudation. This is because  
15 the nuclide concentration reflects the residence time of the material near the land  
16 surface, where it is subject to cosmic ray irradiation (Lal, 1991). The shorter the  
17 residence time, the lower the steady-state equilibrium concentrations of nuclides will be  
18 in minerals within the rock, implying rapid denudation of the landform.

19           The application of the cosmogenic nuclide method was initially confined to  
20 areas of bare rock at high latitudes or in arid environments, but has rapidly spread to  
21 humid and temperate mid-latitude areas where soils cover most of the land surface.  
22 Although the soil thickness in a given region generally ranges from only several  
23 decimeters to several meters, the soil layer provides the key to understanding ongoing  
24 geomorphic and geochemical processes in mountainous terrain. The conversion of

1 bedrock to soil leads to the accumulation of unstable material on hillslopes, thereby  
2 controlling the sediment yield within watersheds, which in turn affects natural  
3 ecosystems in the catchments of mountain streams and the lifetimes of civil engineering  
4 structures in the lower reaches of rivers. At a longer timescale, the soil layer functions  
5 as a geochemical subsystem that consumes atmospheric CO<sub>2</sub> via silicate weathering;  
6 this process possibly acted as a buffer to fluctuations in paleoclimate, having a negative  
7 feedback in terms of weakening the greenhouse effect (Walker et al., 1981; Berner,  
8 1995).

9         The present paper highlights recent advances and future potential of the  
10 cosmogenic nuclide approach in studies of hillslope denudation. Several recent studies  
11 have developed the methodology for quantifying long-term chemical weathering in  
12 soil-mantled hillslopes by combining measurements of cosmogenic nuclides with a  
13 conservative element mass-balance approach (Riebe et al., 2001, 2003, 2004; Green et  
14 al., 2006; Burke et al., 2007; Yoo et al., 2007). These studies have demonstrated the  
15 strong coupling of physical and chemical processes in hillslope denudation. The present  
16 study focuses on the saprolite zone, a chemically decomposed layer that occurs beneath  
17 the mobile soil mantle, where the bedrock is set to be physically disintegrated into the  
18 overlying soil layer. The susceptibility of bedrock to chemical decomposition, especially  
19 in terms of the resulting reduction in mechanical strength, is a crucial factor in  
20 determining the rates of physical soil production and transport, and hence subsequent  
21 chemical weathering in soil sections.

22         We propose a semi-empirical model that describes the reduction in mechanical  
23 strength of bedrock and captures a steady-state depth–strength profile in the saprolite  
24 zone. The term ‘strength’ is here defined as the mechanical resistance of landform

1 materials to physical geomorphic agents, including shearing by gravity or water flow,  
2 freeze–thaw action, bioturbation, and wetting–drying processes. The proposed model  
3 provides a means of evaluating the controlling mechanisms of soil production functions,  
4 linking geologic, climatic, and tectonic factors with the rates of physical and chemical  
5 denudation of soil-mantled hilly landscapes.

6

## 7 **2. Methods for quantifying physical and chemical processes on hillslopes**

8         The denudation of hillslopes progresses via two types of mass loss: (1)  
9 chemical weathering (mineral dissolution by water–rock reactions), and (2) physical  
10 erosion (the mechanical breakdown of bedrock and the downslope removal of the  
11 resulting mineral fragments). These processes act together in developing soil-mantled  
12 hillslopes. The chemical weathering rates were typically measured by solute fluxes from  
13 watersheds (e.g., White and Blum, 1995), or by chemical composition of non-eroding  
14 soils with known age (e.g., Brimhall and Dietrich, 1987). For a physically eroding soil  
15 on a sloping terrain, quantification of the chemical weathering rate requires the mean  
16 residence time of the soil that correlates inversely with the rate of rock-to-soil  
17 conversion, which in turn is equivalent to the long-term rate of total denudation of the  
18 hillslope (White et al., 1998; Anderson et al., 2002).

19         The concentration of cosmogenic nuclides in rock minerals is a function of the  
20 total denudation on a given hillslope (sum of the chemical and physical mass losses).  
21 Denudation rates determined from cosmogenic nuclides are typically averaged over a  
22 timescale of  $10^3$ – $10^5$  yr that is relevant to the timescales for soil generation and  
23 alternation on hillslopes under a wide range of climate regimes. Riebe et al. (2001,  
24 2003) proposed a methodology for separately quantifying the rates of chemical

1 weathering and physical erosion by combining the cosmogenically determined  
2 denudation rate with the geochemical mass balance for a hillslope.

3 Figure 1 shows denudation processes in a soil-mantled mountainous watershed.  
4 Immobile parent material (saprolite on fresh bedrock) is converted to mobile soil on a  
5 hillslope at the rate of  $D$ , and the soil is subject to physical erosion  $E$  and chemical  
6 weathering  $W$  (each of these terms are given in mass flux:  $\text{g m}^{-2} \text{yr}^{-1}$ ). Under  
7 steady-state soil production and denudation, implying a constant soil thickness on the  
8 hillslope over time, the rate of saprolite conversion to soil is equal to the total  
9 denudation (Riebe et al., 2001):

$$10 \quad D = E + W . \quad (1)$$

11 **Fig. 1**

12 Because bedrock subject to denudation contains both soluble and insoluble  
13 components, chemical depletion of the rock-forming minerals should lead to an  
14 enrichment in insoluble elements within soil sections (Fig. 1). Focusing on an insoluble  
15 element such as zirconium, the mass conservation equation can be rewritten as

$$16 \quad D[\text{Zr}]_{\text{rock}} = E[\text{Zr}]_{\text{soil}} , \quad (2)$$

17 where  $[\text{Zr}]_{\text{rock}}$  and  $[\text{Zr}]_{\text{soil}}$  are the concentrations of zirconium in the rock and soil,  
18 respectively (Riebe et al., 2001). Equation (2) states that the zirconium budget during  
19 the conversion of rock to soil is balanced solely with physical erosion, under conditions  
20 of no chemical dissolution. Substitution of Eq. (2) into Eq. (1) yields

$$21 \quad \frac{W}{D} = \left( 1 - \frac{[\text{Zr}]_{\text{rock}}}{[\text{Zr}]_{\text{soil}}} \right) , \quad (3)$$

22 indicating that we are able to quantify the contribution of chemical weathering to total

1 denudation based on the enrichment of conservative elements in soil sections. The ratio  
2 ( $W/D$ ) was termed the chemical depletion fraction (CDF) by Riebe et al. (2003).

3 At a catchment-averaged scale, the total denudation rate  $D$  can be determined  
4 from the cosmogenic nuclide concentration  $C$  in well-mixed sediment washed out from  
5 the source area (Fig. 1). The nuclide concentration  $C$  (atoms  $\text{g}^{-1}$ ) in the sediment can be  
6 written as

$$7 \quad C = \frac{P\Lambda}{D}, \quad (4)$$

8 where  $P$  is the nuclide production rate (atoms  $\text{g}^{-1} \text{yr}^{-1}$ ) at the land surface in the source  
9 area and  $\Lambda$  is the cosmic ray attenuation length ( $\text{g m}^{-2}$ ) (Granger et al., 1996). Equation  
10 (4) is based on the three main assumptions: 1) the hillslopes are eroded continuous  
11 processes, 2) the time required to remove materials with a thickness equivalent to  $\Lambda$   
12 from the hillslopes is much shorter than the radioactive mean life ( $10^6$  yr timescale for  
13  $^{10}\text{Be}$  and  $^{26}\text{Al}$ ), and 3) hillslopes in the source area contribute sediment to the channel in  
14 proportion to their local erosion rate.

15 Combining Eqs. (3) and (4), we can deduce the chemical weathering rate:

$$16 \quad W = \frac{P\Lambda}{C} \left( 1 - \frac{[\text{Zr}]_{\text{rock}}}{[\text{Zr}]_{\text{soil}}} \right). \quad (5)$$

17 Riebe et al. (2004) applied this methodology to several granitic sites in Central and  
18 North America and New Zealand under various climatic and tectonic settings. They  
19 empirically formulated the rates of chemical weathering with the product of an  
20 Arrhenius-like function of mean annual temperature and power functions of the rates of  
21 precipitation and total denudation. The empirical function was successful in explaining  
22 regional variations in the rates of chemical weathering of bulk soils (from close to 0 to  
23  $2 \times 10^2 \text{ g m}^{-2} \text{ yr}^{-1}$ ).

1

### 2 **3. Importance of reductions in bedrock strength**

3 Riebe et al. (2004) concluded that the most crucial factor in controlling the rate  
4 of chemical weathering is the total denudation rate, which in turn is regulated mainly by  
5 tectonic forcing leading toward a local base-level lowering (Riebe et al., 2000); while  
6 the climatic factors appear to affect the relative contribution of chemical weathering  
7 (CDF:  $W/D$ ). Under a given climate, they found that the rate of chemical weathering is  
8 almost proportional to the total denudation rate (rate of rock-to-soil conversion on  
9 hillslopes). This situation is termed ‘supply-limited weathering’, whereby chemical  
10 depletion occurs only if attackable mineral surfaces are made available as a  
11 consequence of the mechanical disintegration of bedrock (Riebe et al., 2004).

12 Riebe et al.’s (2001, 2003, 2004) method enables us to make rough  
13 comparisons of the rates of chemical weathering under different conditions of physical  
14 erosion rates, and suggests a large-scale coupling of chemical and physical processes.  
15 This spatially averaged estimate of the rate of chemical weathering is only valid if the  
16 soil chemistry is homogeneous within the hillslope of interest, implying uniform  
17 mineral supply, soil transport, and subsurface water dynamics regardless of topographic  
18 location. However, most recent studies suggest that CDFs and chemical weathering  
19 rates vary at the hillslope scale because of spatial variations in soil production rates, soil  
20 particle dwell time, and fluid flux (Green et al., 2006; Burke et al., 2007). Point-specific  
21 CDFs and chemical weathering rates have been modeled by integrating physical soil  
22 production and transport along a hillslope transect (Yoo et al., 2007).

23 Soil production is one of the most crucial factors in modeling local variations  
24 in the values of CDF and the rates of chemical weathering (Yoo et al., 2007). Heimsath

1 et al. (1997) determined the first empirical soil production function from measurements  
2 of cosmogenic nuclides at the soil–saprolite boundary, assuming the steady-state  
3 production and transport of soil on the hillslope. Heimsath et al. (1997, 1999, 2000,  
4 2001a, b, 2005, 2006) deduced the soil production functions at several sites in northern  
5 California, U.S., and Southeast Australia, and demonstrated that the soil production rate  
6 decreases exponentially with increasing local soil depth (Fig. 2). The intercept of the  
7 soil production function showed marked differences among the sites analyzed, varying  
8 between 50 and 300 mm kyr<sup>-1</sup> (Fig. 2).

## 9 Fig. 2

10 The balance between mechanical strength and the physical processes acting on  
11 a hillslope determines whether a block of bedrock disintegrates into loose mineral  
12 fragments; consequently, differences in the soil production functions should be  
13 considered with respect to the strength reduction behavior of bedrock and the threshold  
14 of physical erosion. A reduction in strength occurs within the saprolite zone: a  
15 decomposed layer between soil and fresh bedrock. In the present study, we suggest the  
16 potential of combining analyses of cosmogenic nuclides at the soil–saprolite boundary  
17 and determining a strength profile for the saprolite zone in terms of quantifying the  
18 sensitivity of bedrock to strength reduction, as this sensitivity is a crucial factor in  
19 determining the physical erodibility of saprolite and hence the rates of soil production  
20 and soil chemical weathering on a hillslope.

21

## 22 **4. Model for quantifying the reduction in rock strength**

23 In this section, we present a semi-empirical model that describes the reduction  
24 in the mechanical strength of bedrock during weathering. Three subsurface layers are

1 defined within a hillslope (Fig. 3): the mobile soil layer above the depth of the  
 2 soil–saprolite boundary  $Z_{SSB}$  [L], the zone of fresh bedrock below the depth of the  
 3 weathering front  $Z_{WF}$  [L], and the layer of saprolite between  $Z_{SSB}$  and  $Z_{WF}$ . The depth  $Z$   
 4 [L] is defined normal to the land surface, being equal to zero at the land surface at an  
 5 arbitrary point in time. The depth  $Z_{SSB}$  is the boundary between the mobile and  
 6 immobile layers. No strength reduction occurs below  $Z_{WF}$ , beyond the extent of  
 7 weathering.

8 **Fig. 3**

9 Under conditions of steady-state denudation on a hillslope, the soil–saprolite  
 10 boundary and the weathering front migrate downward at the same rate. Assuming that  
 11 the total denudation rate in the soil section is  $D$  [ $M L^{-2} T^{-1}$ ], the rate of downward  
 12 migration of the soil–saprolite boundary is  $D/\rho_{sp}$  [ $L T^{-1}$ ], where  $\rho_{sp}$  [ $M L^{-3}$ ] is the  
 13 density of saprolite. The rate  $D/\rho_{sp}$  is the same for downward penetration of the  
 14 weathering front, fulfilling the condition that the hillslope maintains a constant  
 15 thickness of soil and saprolite layers over time (Fig. 3).

16 The strength of fresh bedrock  $S_{FB}$  [ $M L^{-1} T^{-2}$ ] decreases to the erosion  
 17 threshold  $S_{ET}$  [ $M L^{-1} T^{-2}$ ] within the saprolite zone, leading to mechanical disintegration  
 18 and the removal of material at the uppermost face of the saprolite. The reduction in rock  
 19 strength  $S$  [ $M L^{-1} T^{-2}$ ] with time  $t$  [T] has been modeled previously by Sunamura  
 20 (1996):

$$21 \quad \frac{dS}{dt} = -kS \quad (6)$$

22 where  $k$  [ $T^{-1}$ ] is the strength reduction coefficient ( $k > 0$ ). The equation's prediction of  
 23 an exponential decrease in rock strength with time has been verified by measurements  
 24 of the compressive and tensile strength of rhyolite lavas with eruption ages of 40, 20,

1 2.6, and 1.1 ka (Oguchi, 1999).

2 This study assumes that the strength reduction coefficient  $k$  decreases with  
3 increasing depth within the saprolite zone, as an inward decrease in the degree of  
4 weathering is commonly observed in subsurface hillslope profiles. The rate of strength  
5 reduction must be zero below the weathering front. Accordingly, the coefficient  $k$  should  
6 be a depth-dependent value that decreases with increasing depth below  $Z_{SSB}$  and  
7 diminishes to zero at  $Z \rightarrow Z_{WF}$ :

$$8 \quad k = f(Z) = m \left( 1 - \frac{Z}{Z_{WF}} \right)^{n-1} \quad (Z_{SSB} \leq Z < Z_{WF}), \quad (7)$$

9 where  $m$  [ $T^{-1}$ ] and  $n$  [-] are parameters ( $m > 0$ ;  $n \geq 1$ ) that represent the sensitivity of  
10 bedrock to strength reductions with time and depth, respectively.

11 The apparent profile of subsurface strength should be time-independent under  
12 steady-state denudation, characterized by a constant thickness of soil and saprolite. Thus,  
13 the strength reduction with time at depth  $Z$  should be zero (note that  $Z$  is the depth from  
14 the eroding land surface at an arbitrary point in time):

$$15 \quad \frac{\partial S}{\partial t} = -m \left( 1 - \frac{Z}{Z_{WF}} \right)^{n-1} S + \frac{D}{\rho_{sp}} \frac{\partial S}{\partial Z} = 0. \quad (8)$$

16 The solution of the differential equation is

$$17 \quad S = S_{FB} \exp \left[ -\frac{m \rho_{sp}}{n D} Z_{WF} \left( 1 - \frac{Z}{Z_{WF}} \right)^n \right] \quad (Z_{SSB} \leq Z < Z_{WF}), \quad (9)$$

18 with the initial condition that  $\lim_{Z \rightarrow Z_{WF}} S = S_{FB}$ .

19 The three curves shown in Fig. 3 represent schematic strength profiles in the  
20 cases of  $n = 1, 2,$  and  $3$ . A depth–strength profile for a given saprolite zone, along with

1 values of  $S_{FB}$ ,  $Z_{WF}$ , and  $\rho_{sp}$ , can be determined from field- and laboratory-based  
 2 investigations, and the denudation rate  $D$  can be deduced from cosmogenic nuclide  
 3 analyses at  $Z_{SSB}$ . Thus, fitting Eq. (9) to the measured depth–strength profile provides  
 4 the optimal values of  $m$  and  $n$  in the strength reduction function.

5 The strength  $S$  decreases to the erosion threshold  $S_{ET}$  at  $Z = Z_{SSB}$  (Fig. 3); that  
 6 is,

$$7 \quad S_{ET} = S_{FB} \exp \left[ -\frac{m \rho_{sp}}{n D} Z_{WF} \left( 1 - \frac{Z_{SSB}}{Z_{WF}} \right)^n \right]. \quad (10)$$

8 Solving Eq. (10) for  $D$  gives

$$9 \quad D = \rho_{sp} \frac{m}{n} \frac{H_{sp}^n}{Z_{WF}^{n-1}} \left[ \ln \left( \frac{S_{FB}}{S_{ET}} \right) \right]^{-1}, \quad (11)$$

10 where  $H_{sp}$  [L] is the steady-state thickness of saprolite ( $H_{sp} = Z_{WF} - Z_{SSB}$ ). The value of  
 11  $H_{sp}$  can be obtained via observations of drill core from the hillslope of interest or  
 12 outcrop exposed within a large quarry if present, while  $S_{ET}$  can be deduced from  
 13 strength measurements at the soil–saprolite boundary. Consequently, we can test the  
 14 strength reduction model using Eq. (11), provided that denudation rates  $D$  are available  
 15 at several points on a hillslope with contrasting  $H_{sp}$  and  $S_{ET}$ .

16 It is possible to use various measures of material strength (e.g., compressive or  
 17 tensile strength, cohesion) and proxies (e.g., dynamic cone penetrating resistance, static  
 18 cone or needle penetration hardness, vane shearing strength, rebound values of an  
 19 impact test hammer) in this approach. An appropriate strength measure or proxy should  
 20 be analyzed to understand geomorphic processes with respect to the type of driving  
 21 forces operating on the landform material subject to erosion; however, a single measure  
 22 or proxy is seldom able to cover the wide range in strength of diverse landform

1 materials that vary from fresh, hard bedrock to soft, loose saprolite and soil. Although  
2 practical difficulties remain in terms of measuring material strength, the proposed model  
3 provides a conceptual framework in which to quantify the strength reduction function of  
4 bedrock.

5 Lithologic, climatic, and topographic factors act to regulate the values of  
6 parameters employed in the proposed model. The strength of fresh bedrock  $S_{FB}$  varies  
7 for different rock types, and the parameters  $m$ ,  $n$ , and  $H_{sp}$  are controlled by the solubility  
8 of bedrock (which varies with mineral composition) and slope hydrology or climate  
9 conditions. The erosion threshold  $S_{ET}$  is influenced by the local hillslope gradient,  
10 thickness of the soil mantle, and the intensity and type of physical processes that operate  
11 at the soil–saprolite boundary. Testing of the strength reduction model using Eqs. (9)  
12 and (11) under diverse environments would provide clues to the controlling mechanisms  
13 of the rates of soil production and transport, and hence the rate of chemical weathering  
14 on hillslopes.

15

## 16 **5. Concluding remarks**

17 The concentration of cosmogenic nuclides at the soil–saprolite boundary  
18 reflects the duration over which the fresh bedrock converts to a mobile soil layer, and  
19 therefore the time required for the bedrock strength to decrease to the threshold of  
20 physical erosion within the saprolite zone. The model proposed in this study can be used  
21 to evaluate the susceptibility of bedrock to strength reduction with time and depth,  
22 providing crucial data for understanding the rate of rock-to-soil conversion on hillslopes  
23 and hence the rate of chemical weathering in soil sections. Although the proposed  
24 model is semi-empirical and based on the assumption of steady-state conditions, it

1 provides a new theoretically motivated soil-production function, expressed as Eq. (11).  
2 The model requires cosmogenically determined denudation rates and several other  
3 parameters that are readily obtainable from field- and laboratory-based investigations.  
4 Future testing of the model within various climatic, tectonic, and lithologic settings is  
5 likely to reveal the mechanisms that control the rates of soil production and chemical  
6 weathering on hillslopes, as well as those factors that influence landscape diversity such  
7 as the development of soil-mantled or bare-rock-dominated hilly terrains.

8

### 9 **Acknowledgments**

10 Thoughtful comments from two anonymous reviewers greatly improved the  
11 manuscript. This research was supported financially by a Grant-in-Aid for Scientific  
12 Research (B 19300305, principal investigator: Y. Matsukura) and a Grant-in-Aid for  
13 JSPS Fellows (PD 19-1748) held by Y. Matsushi.

14

### 15 **References**

- 16 Anderson, S.P., Dietrich, W.E., Brimhall, G.H., 2002. Weathering profiles, mass-balance  
17 analysis, and rates of solute loss: linkages between weathering and erosion in a  
18 small, steep catchment. *Geological Society of America Bulletin* 114, 1143–1158.
- 19 Berner, R.A., 1995. Chemical weathering and its effect on atmospheric CO<sub>2</sub> and climate.  
20 In: White, A.F., Brantley, S.L. (Eds.), *Chemical Weathering Rates of Silicate*  
21 *Minerals. Reviews in Mineralogy* 31, Mineralogical Society of America,  
22 Washington, D.C., pp. 565–583.
- 23 Bierman, P.R., Caffee, M.W., Davis, P.T., Marsella, K., Pavich, M., Colgan, P.,  
24 Mickelson, D., Larsen, J., 2002. Rates and timing of earth surface processes from *in*

- 1        *situ*-produced cosmogenic Be-10. In: Grew, E.S. (Ed.), Beryllium: Mineralogy,  
2        petrology, and geochemistry. Reviews in Mineralogy and Geochemistry 50,  
3        Mineralogical Society of America, Washington, D.C., pp. 147–205.
- 4        Bierman, P.R., Nichols, K.K., 2004. Rock to sediment—Slope to sea with  $^{10}\text{Be}$ —Rates  
5        of landscape change. Annual Review of Earth and Planetary Sciences 32, 215–255.
- 6        Brimhall, G.H., Dietrich, W.E., 1987. Constitutive mass balance relations between  
7        chemical composition, volume, density, porosity, and strain in metasomatic  
8        hydrochemical systems: results on weathering and pedogenesis. Geochimica et  
9        Cosmochimica Acta 51, 567–587.
- 10        Burke, B.C., Heimsath, A.M., White, A.F., 2007. Coupling chemical weathering with  
11        soil production across soil-mantled landscapes. Earth Surface Processes and  
12        Landforms 32, 853–873.
- 13        Cockburn, H.A.P., Summerfield, M.A., 2004. Geomorphological applications of  
14        cosmogenic isotope analysis. Progress in Physical Geography 28, 1–42.
- 15        Gosse, J.C., Phillips, F.M., 2001. Terrestrial *in situ* cosmogenic nuclides: theory and  
16        application. Quaternary Science Reviews 20, 1475–1560.
- 17        Granger, D.E., Kirchner, J.W., Finkel, R., 1996. Spatially averaged long-term erosion  
18        rates measured from *in situ*-produced cosmogenic nuclides in alluvial sediment.  
19        Journal of Geology 104, 249–257.
- 20        Green, E.G., Dietrich, W.E., Banfield, J.F., 2006. Quantification of chemical weathering  
21        rates across an actively eroding hillslope. Earth and Planetary Science Letters 242,  
22        155–169.
- 23        Heimsath, A.M., Dietrich, W.E., Nishiizumi, K., Finkel, R.C., 1997. The soil production  
24        function and landscape equilibrium. Nature 388, 358–361.

- 1 Heimsath, A.M., Dietrich, W.E., Nishiizumi, K., Finkel, R.C., 1999. Cosmogenic  
2 nuclides, topography, and the spatial variation of soil depth. *Geomorphology* 27,  
3 151–172.
- 4 Heimsath, A.M., Chappell, J., Dietrich, W.E., Nishiizumi, K., Finkel, R.C., 2000. Soil  
5 production on a retreating escarpment in southeastern Australia. *Geology* 28,  
6 787–790.
- 7 Heimsath, A.M., Dietrich, W.E., Nishiizumi, K., Finkel, R.C., 2001a. Stochastic  
8 processes of soil production and transport: erosion rates, topographic variation and  
9 cosmogenic nuclides in the Oregon Coast Range. *Earth Surface Processes and*  
10 *Landforms* 26, 531–552.
- 11 Heimsath, A.M., Chappell, J., Dietrich, W.E., Nishiizumi, K., Finkel, R.C., 2001b. Late  
12 Quaternary erosion in southeastern Australia: a field example using cosmogenic  
13 nuclides. *Quaternary International* 83–85, 169–185.
- 14 Heimsath, A.M., Furbish, D.J., Dietrich, W.E., 2005. The illusion of diffusion: field  
15 evidence for depth-dependent sediment transport. *Geology* 33, 949–952.
- 16 Heimsath, A.M., Chappell, J., Finkel, R.C., Fifield, K., Alimanovic, A., 2006.  
17 Escarpment erosion and landscape evolution in southeastern Australia. In: Willett,  
18 S.D., Hovius, N., Brandon, M.T., Fisher, D.M. (Eds.), *Tectonics, Climate, and*  
19 *Landscape Evolution*. Geological Society of America Special Paper 398, Geological  
20 Society of America, Boulder, CO, pp. 173–190.
- 21 Lal, D., 1991. Cosmic ray labeling of erosion surfaces: *in situ* nuclide production rates  
22 and erosion models. *Earth and Planetary Science Letters* 104, 424–439.
- 23 Oguchi, C.T., Hatta, T., Matsukura, Y., 1999. Weathering rates over 40,000 years based  
24 on changes in rock properties of porous rhyolite. *Physics and Chemistry of the Earth*

- 1 (A) 24, 861–870.
- 2 Riebe, C.S., Kirchner, J.W., Granger, D.E., Finkel, R.C., 2000. Erosional equilibrium  
3 and disequilibrium in the Sierra Nevada, inferred from cosmogenic  $^{26}\text{Al}$  and  $^{10}\text{Be}$  in  
4 alluvial sediment. *Geology* 28, 803–806.
- 5 Riebe, C.S., Kirchner, J.W., Granger, D.E., Finkel, R.C., 2001. Strong tectonic and weak  
6 climatic control of long-term chemical weathering rates. *Geology* 29, 511–514.
- 7 Riebe, C.S., Kirchner, J.W., Finkel, R.C., 2003. Long-term rates of chemical weathering  
8 and physical erosion from cosmogenic nuclides and geochemical mass balance.  
9 *Geochimica et Cosmochimica Acta* 67, 4411–4427.
- 10 Riebe, C.S., Kirchner, J.W., Finkel, R.C., 2004. Erosional and climatic effects on  
11 long-term chemical weathering rates in granitic landscapes spanning diverse climate  
12 regimes. *Earth and Planetary Science Letters* 224, 547–562.
- 13 Sunamura, T., 1996. A physical model for the rate of coastal tafoni development.  
14 *Journal of Geology* 104, 741–748.
- 15 Von Blanckenburg, F., 2006. The control mechanisms of erosion and weathering at  
16 basin scale from cosmogenic nuclides in river sediment. *Earth and Planetary Science*  
17 *Letters* 242, 224–239.
- 18 Walker, J.C.G., Hays, P.B., Kasting, J.F., 1981. A negative feedback mechanism for the  
19 long-term stabilization of Earth's surface temperature. *Journal of Geophysical*  
20 *Research* 86 (C10), 9776–9782.
- 21 White, A.F., Blum, A.E., 1995. Effects of climate on chemical weathering in watersheds.  
22 *Geochimica et Cosmochimica Acta* 59, 1729–1747.
- 23 White, A.F., Blum, A.E., Schulz, M.S., Vivit, D.V., Stonestrom, D.A., Larsen, M.,  
24 Murphy, S.F., Eberl, D., 1998. Chemical weathering in a tropical watershed,

1        Luquillo Mountains, Puerto Rico: I. long-term versus short-term weathering fluxes.  
2        *Geochimica et Cosmochimica Acta* 62, 209–226.  
3    Yoo, K. Amundson, R., Heimsath, A.M., Dietrich, W.E., Brimhall, G.H., 2007.  
4        Integration of geochemical mass balance with sediment transport to calculate rates  
5        of soil chemical weathering and transport on hillslopes. *Journal of Geophysical*  
6        *Research* 112, F02013.

1 **Figure captions**

2

3 Fig. 1. Schematic illustration of denudation processes within a soil-mantled watershed.  
4  $D$ : rate of conversion of bedrock to soil;  $E$ : rate of physical erosion;  $W$ : rate of chemical  
5 weathering;  $P$ : production rate of cosmogenic nuclides;  $C$ : cosmogenic nuclide  
6 concentration;  $A$ : cosmic ray attenuation length.

7

8 Fig. 2. Plot showing the exponential decrease in soil production rates with increasing  
9 soil thickness, as reported in Heimsath et al. (1997, 1999: Marin County, CA, US;  
10 2001a: Coos Bay, OR, US; 2005: Point Reyes, CA, US; 2000, 2001b, 2006: Bega Basin,  
11 Southeast Australia). The soil production functions were determined based on analyses  
12 of cosmogenic nuclides at the soil–saprolite boundary, assuming steady-state conditions  
13 of the formation and transport of soil upon each of the analyzed hillslopes. The shaded  
14 regions in the figure indicate the range of uncertainty based on variance-weighted  
15 regressions for datasets of local soil thickness and cosmogenically determined rates of  
16 soil production.

17

18 Fig. 3. Subsurface layers and model strength profiles for a soil-mantled hillslope. The  
19 strength of fresh bedrock  $S_{FB}$  decreases to the erosion threshold  $S_{ET}$  within the saprolite  
20 zone. Both the soil–saprolite boundary and the weathering front migrate downward at  
21 the rate of  $D/\rho_{sp}$  (where  $\rho_{sp}$  is the density of saprolite), thereby fulfilling the condition  
22 that the hillslope maintains soil and saprolite layers of constant thickness over time, as  
23 well as a constant apparent strength profile. The strength reduction functions are  
24 modeled as Eqs. (6) to (9) in the text.

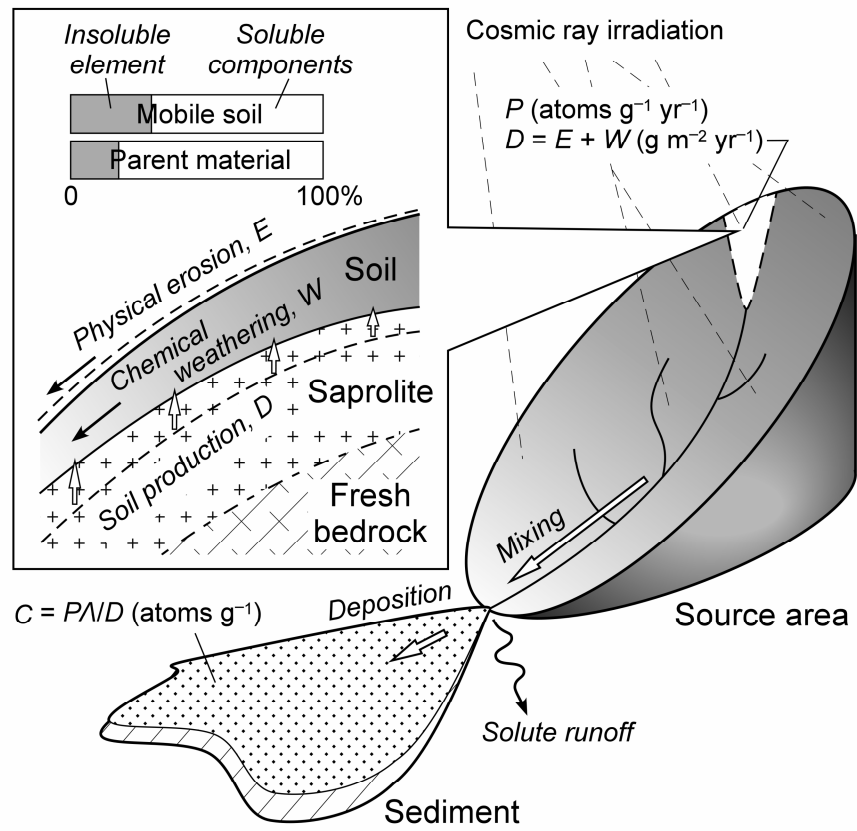


Fig. 1

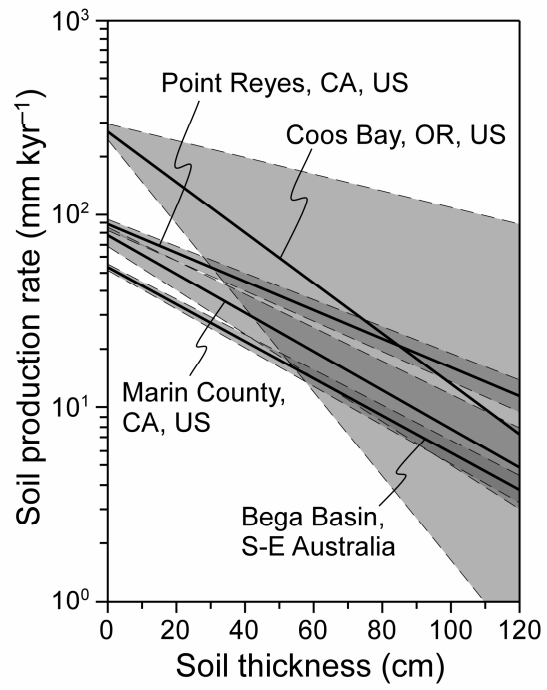


Fig. 2

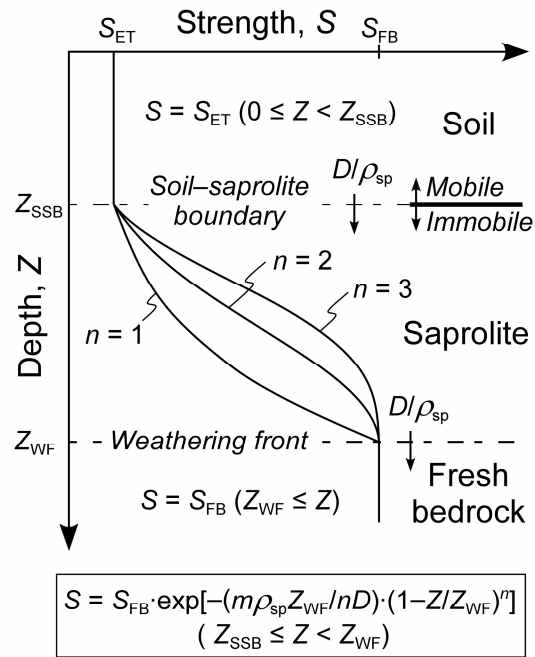


Fig. 3